

# Base-Pairing Directed Folding of a Bimolecular G-Quadruplex: New Insights into G-Quadruplex-Based DNazymes

Tao Li, Erkang Wang, and Shaojun Dong\*[a]

G-rich DNA sequences are able to fold into intramolecular or intermolecular four-stranded structures known as G-quadruplexes.<sup>[1–3]</sup> Such DNA structures consist of at least two consecutive G-tetrads (a planar arrangement of four guanine bases hydrogen-bonded to each other).<sup>[4]</sup> The strong van der Waals attractions between adjacent G-tetrads allow the formation of stable DNA G-quadruplexes in the presence of coordinating cations, especially  $K^+$ . For a unimolecular or bimolecular G-quadruplex, the stacked G-tetrads are generally linked by nucleic acid loops. In some cases, different loop residues are able to be hydrogen-bonded as well,<sup>[5]</sup> contributing to the stability of the G-quadruplex.<sup>[6]</sup> Furthermore, base-pairing can be utilized to direct or confine the folding of G-quadruplexes. Appending an appropriate base-pairing duplex to the G-quadruplex motif may confer better properties (e.g. structural stability and ligand-binding affinity).<sup>[6–8]</sup> Accordingly, it is significant and interesting to investigate the influence of base-pairing on the properties of G-quadruplexes.

DNazymes are non-natural nucleic acid enzymes that have shown their great potential as biocatalysts for many biochemical reactions.<sup>[9–11]</sup> An interesting kind of DNazymes formed by G-quadruplex DNA aptamers (e.g. PS2M)<sup>[12,13]</sup> displays peroxidase-like activity. Such G-quadruplex-based DNazymes can effectively catalyze the  $H_2O_2$ -mediated oxidation of 2,2'-azino-bis(3-ethylbenzothiazoline-6-sulfonic acid)diammonium salt (ABTS)<sup>[14,15]</sup> or luminol,<sup>[16]</sup> enabling them to serve as the catalytic labels (or beacons)

for biomolecule detection.<sup>[14,15,17–20]</sup> An intermolecular G-quadruplex consisting of two G-rich single-stranded DNAs is also able to form an effective DNzyme with hemin.<sup>[21]</sup> This bimolecular G-quadruplex is found to exhibit an enhanced DNzyme function after treatment with the complementary DNA of its two free nucleic acid parts.<sup>[14]</sup> This suggests that base pairs flanking the G-quadruplex motif contribute to the formation of the DNzyme, providing evidence for the design of G-quadruplex-based DNazymes with improved properties.

Herein we report on the base-pairing directed folding of a bimolecular G-quadruplex. By appending a base-pairing duplex to the G-quadruplex motif, different folding topologies of the bimolecular G-quadruplex are confined, depending on the position of the base pairs. Interestingly, these bimolecular structures exhibit similar hemin-binding affinities, whereas their DNzyme functions are entirely different. In particular, three T–A base pairs on the 5'-terminals of the G-quadruplex confer the best DNzyme function ever reported. These findings reveal an important intrinsic role of additional base pairs in the G-quadruplex structure, and provide a clue to the formation mechanism of the G-quadruplex-based DNzyme.

Two G-rich single-stranded DNAs d(GGGACGGG) and d(GTGGAGGG), here designated as S8-1 and S8-2, were chosen as the models. In the presence of coordinating cations, these two DNAs are able to fold into a bimolecular G-quadruplex (herein referred to as G4-2S8). After incubation with hemin, G4-2S8 gives rise to a clear hyperchromicity of the Soret band (Figure 1A), which is consistent with the hemin–G-quadruplex interaction.<sup>[12,13]</sup> Binding assays reveal that G4-2S8 binds hemin with a supramicromolar affinity ( $K_d = 3.93 \mu M$ ). Like other G-quadruplex-based DNazymes, the hemin–G4-2S8 complex is found to catalyze the  $H_2O_2$ -mediated oxidation of ABTS. The reaction product, that is, the cationic free radical  $ABTS^{\bullet+}$ , has a maximal absorption at about 420 nm ( $\epsilon = 3.6 \times 10^4 L mol^{-1} cm^{-1}$ ). At this wavelength, a time-dependent increase in absorbance is observed (Figure 1B), revealing a modest catalytic activity (the initial rate  $\nu = 5.88 \mu M min^{-1}$ ) of 0.5  $\mu M$  hemin–G4-2S8. This enables

[a] T. Li, Prof. Dr. E. Wang, Prof. S. Dong  
State Key Laboratory of Electroanalytical Chemistry  
Changchun Institute of Applied Chemistry  
Chinese Academy of Sciences  
Changchun, Jilin, 130022 (China)  
and  
Graduate School of the Chinese Academy of Sciences  
Beijing, 100039 (China)  
Fax: (+86) 431-85689711  
E-mail: dongsj@ciac.jl.cn

Supporting information for this article is available on the WWW under <http://dx.doi.org/10.1002/chem.200801825>.

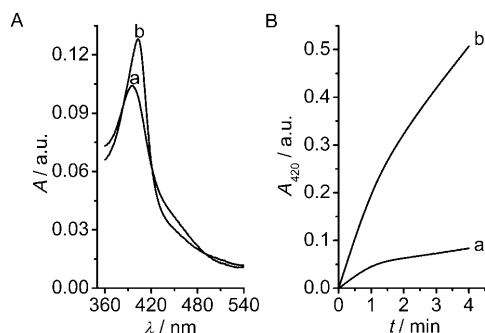
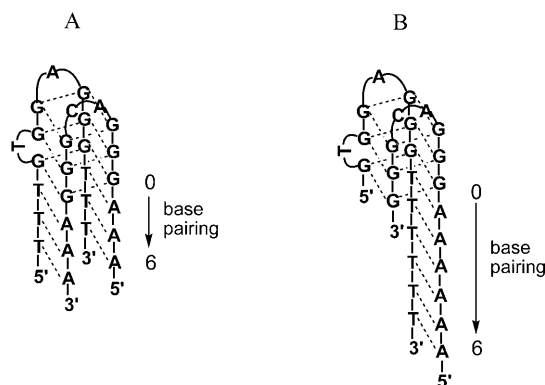


Figure 1. Spectroscopic analysis of the hemin-binding affinity and DNAzyme function of G4-2S8: a) Uncomplexed hemin, b) after incubation with G4-2S8. A) UV/Vis absorption spectra for analyzing the interaction between 1  $\mu$ M hemin and 4  $\mu$ M G4-2S8 in the binding buffer consisting of 25 mM HEPES (pH 8.0), 20 mM KCl, 200 mM NaCl, 0.05 % (w/v) Triton X-100, and 1 % (v/v) DMSO. B) Reaction kinetics of the  $\text{H}_2\text{O}_2$ -mediated oxidation of ABTS catalyzed by 0.5  $\mu$ M catalysts. Absorbance was monitored at 420 nm in the detection buffer consisting of 5.4 mM ABTS, 0.6 mM  $\text{H}_2\text{O}_2$ , 25 mM HEPES (pH 8.0), 20 mM KCl, 200 mM NaCl, 0.05 % Triton X-100, and 1 % DMSO.

a spectroscopic investigation of the influence of additional base pairs flanking the G-quadruplex motif.

Scheme 1 depicts two cases of appending a different number of T–A base pairs to the bimolecular G-quadruplex G4-2S8. This G-quadruplex allows the introduction of at



Scheme 1. Formation of base pairs across the grooves of bimolecular G-quadruplex G4-2S8. A) A different number of T–A base pairs is appended on the two flanks of G4-2S8. B) The appended T–A base pairs are located on only one flank of G4-2S8. See the color version in the Supporting Information.

most two additional base-pairing duplexes. The appended base pairs are hydrogen-bonded across the G-quadruplex grooves, which have potential influence on the intrinsic properties of the G-quadruplex. This is reflected by the remarkable changes in the DNAzyme function of G4-2S8 after the introduction of additional base-pairing duplexes, as shown in Figure 2.

In the two cases described in Scheme 1, a different influence of additional T–A base pairs on the DNAzyme function of G4-2S8 is observed. When the appended base pairs are located on the two flanks of G4-2S8 (Scheme 1A), the

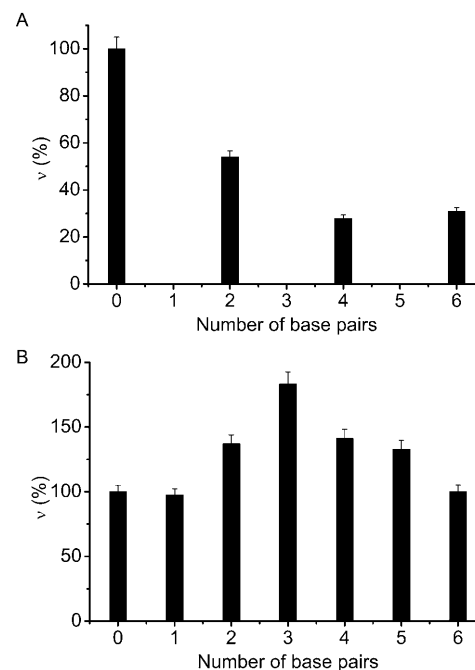


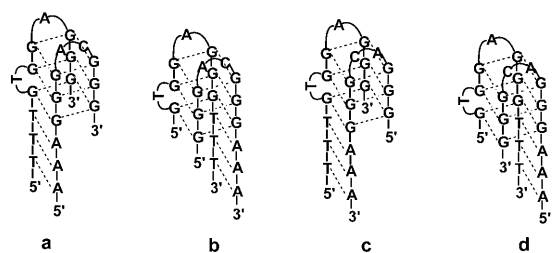
Figure 2. Influence of a different number of additional T–A base pairs on the DNAzyme function of bimolecular G-quadruplex G4-2S8. A) Change of the catalytic activity of 0.5  $\mu$ M hemin-G4-2S8 DNAzyme after appending two base-pairing duplexes to G4-2S8. B) Change of the catalytic activity of 0.5  $\mu$ M hemin-G4-2S8 DNAzyme after appending a different number of base pairs to only one flank of GS8-8. The initial rate ( $v$ ) was determined in the detection buffer (shown in Figure 1B) within the first minute.

introduction of additional base-pairing duplexes results in a gradual decrease in the DNAzyme function of the G-quadruplex (Figure 2A). In contrast, when only one base-pairing duplex is appended to G4-2S8 (Scheme 1B), two–five base pairs flanking the G-quadruplex motif promote the DNAzyme function (Figure 2B). In this case, the DNAzyme activity increases to 183 % as the base-pairing duplex is lengthened to 3 bp, whereas a gradual decrease is observed if more base pairs are appended. The above observations indicate that three T–A base pairs flanking the G-quadruplex motif can promote the DNAzyme function of G4-2S8 to the greatest extent. These phenomena are mainly attributed to the base-pairing directed folding of the G-quadruplex DNA. In our experiments, the formation of base pairs occurs prior to the formation of the G-quadruplex structure (see the Experimental Section). The complementary bases on one terminal (3'- or 5'-terminal) of S8-1 and S8-2 are hydrogen-bonded together, which facilitates and also confines the folding of two single-stranded DNAs into the bimolecular G-quadruplex structure.

To further demonstrate the structural role of additional base pairs in the G-quadruplex, we changed the type of bases, that is, we replaced the base pair T–A by C–G (see Scheme S1 in the Supporting Information). Similarly, the appended C–G base pairs are capable of promoting the DNAzyme function of the G-quadruplex, and their number clearly influences the enzyme activity (see Figure S1 in the Sup-

porting Information). Our experiments were all performed under the same conditions, meaning that our observations are primarily attributed to the change of the intrinsic properties of the G-quadruplex.

The results from Figure 2 inspired us to control the folding topologies of the G-quadruplex by base-pairing. Here S8-1 and S8-2 were also chosen as model DNAs. An additional three-base-pair duplex can direct these two G-rich DNAs to fold into different bimolecular G-quadruplexes with quadruplex/duplex DNA structures (Scheme 2). The



Scheme 2. Base-pairing directed folding topologies of the bimolecular G-quadruplex formed by S8-1 and S8-2. See text for details and the Supporting Information for a color version.

two structures **a** and **b** have the same G-quadruplex motif, and their only difference lies in the position of three T–A base pairs. The same is true for the structures **c** and **d**. These G-quadruplex structures provide access to the spectroscopic investigation on how the base-pairing duplex influences the properties of G-quadruplexes, mainly in terms of hemin-binding affinity and DNAzyme function.

Figure 3 shows the spectroscopic analysis of the hemin-binding affinities and DNAzyme functions of four bimolecular G-quadruplex structures. After incubation with hemin, the structures **a**, **b**, **c**, and **d** give rise to a different degree of hyperchromicity of the Soret band (Figure 3A), indicating the binding of G-quadruplexes to hemin.<sup>[12,13]</sup> Binding assays reveal that these quadruplex/duplex DNA structures bind hemin with similar affinities (Table 1). In comparison with G4-2S8, there is over 2.5-fold improvement in the G-quadruplex affinity after introduction of the additional three-base-pair duplex. However, different phenomena are observed when the DNAzyme functions of G-quadruplexes are investigated (Figure 3B). The structures **a**, **b**, **c**, and **d** are all able to form effective DNAzymes with hemin. These G-quadruplex-based DNAzymes exhibit entirely different catalytic activities towards the H<sub>2</sub>O<sub>2</sub>-mediated oxidation of ABTS (Figure 3B, curves a–d). Table 1 lists the enzymatic reaction rates corresponding to the four G-quadruplex structures. The two structures **a** and **b** with the same G-quadruplex motif have distinct DNAzyme functions, which is attributed to the different position of the base pairs in their structures. The bimolecular structure **a** in which three T–A base pairs are located on the two 5'-terminals possesses the highest DNAzyme function ( $\nu = 23.6 \mu\text{M min}^{-1}$ ) among the four structures, which is higher than that of the reported counterparts such as PS2M<sup>[12,13]</sup> ( $\nu = 18.6 \mu\text{M min}^{-1}$ ). That is, the ap-

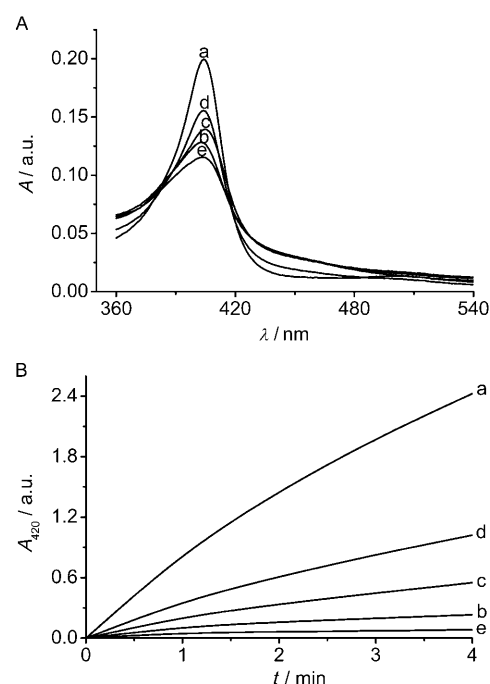


Figure 3. Spectroscopic analysis of the hemin-binding affinities and DNAzyme functions of four quadruplex/duplex DNA structures. Curves a–d represent those for the structures **a**, **b**, **c**, and **d**, and curve e represents the background (uncomplexed hemin). A) UV/Vis absorption spectra for analyzing the interactions between  $1 \mu\text{M}$  hemin and  $4 \mu\text{M}$  bimolecular G-quadruplexes (**a–d**) in the binding buffer. B) Reaction kinetics of the H<sub>2</sub>O<sub>2</sub>-mediated oxidation of ABTS catalyzed by  $0.5 \mu\text{M}$  of hemin–G-quadruplex complexes. Absorbance was monitored at 420 nm in the detection buffer (shown in Figure 1B).

Table 1. The hemin-binding affinities ( $K_d$ ) and DNAzyme functions ( $\nu$ ) of different bimolecular G-quadruplex structures (**a–d**).

Hemin-G-quadruplex DNAzymes	$K_d$ [ $\mu\text{M}$ ] <sup>[a]</sup>	$\nu$ [ $\mu\text{M min}^{-1}$ ] <sup>[b]</sup>
hemin- <b>a</b>	$1.42 \pm 0.19$	23.6
hemin- <b>b</b>	$1.29 \pm 0.17$	3.12
hemin- <b>c</b>	$1.37 \pm 0.12$	5.87
hemin- <b>d</b>	$1.35 \pm 0.07$	10.2

[a] Determined in an aqueous buffer consisting of 5.4 mM ABTS, 0.6 mM H<sub>2</sub>O<sub>2</sub>, 25 mM HEPES (pH 7.4), 20 mM KCl, 200 mM NaCl, 0.05% Triton X-100, and 1% DMSO by using UV/Vis absorption spectroscopy. For more details see the Experimental Section. In these four cases, the RSD for  $K_d$  determination was always less than 10%. [b] Determined at 420 nm with  $\epsilon(\text{ABTS}^+) = 3.6 \times 10^4 \text{ L mol}^{-1} \text{ cm}^{-1}$  in the detection buffer (shown in Figure 1B).

pendent three T–A base pairs on the 5'-terminals of the bimolecular G-quadruplex confer the most excellent DNAzyme function. In contrast, the structure **b** in which the base pairs are on the two 3'-terminals exhibits the lowest DNAzyme function ( $\nu = 3.12 \mu\text{M min}^{-1}$ ), even lower than that of the G-quadruplex G4-2S8 with no base-pairing duplex.

From the above experimental observations two rational conclusions can be made: 1) The appended three T–A base pairs flanking the G-quadruplex motif are favorable for hemin binding, whereas they do not always contribute to the DNAzyme function of the G-quadruplex. 2) The position of

the base-pairing duplex has no obvious effect on the affinity of the G-quadruplex, whereas it dramatically influences the DNAzyme function. These findings provide a clue to the formation mechanism of G-quadruplex-based DNAzymes. In the structure of the hemin–G-quadruplex complex, hemin is generally thought to stack on the terminal G-tetrads.<sup>[22,23]</sup> The guanine residues of terminal G-tetrads, especially those on the 3'-terminals, most possibly supply an axial ligand to the ferric moiety of hemin, just like the histidine residues in protein peroxidases.<sup>[24]</sup> This coordination is crucial for protein peroxidases or G-quadruplex-based DNAzymes and significantly contributes to their excellent enzyme activities, which are much higher than that of the uncomplexed hemin.

In conclusion, we have investigated the base-pairing directed folding of a bimolecular G-quadruplex, and gained some new insights into G-quadruplex-based DNAzymes. Two G-rich single-stranded DNAs were chosen as the models, which are able to fold into a bimolecular G-quadruplex with modest hemin-binding affinity and DNAzyme function. Three appended consecutive T–A base pairs flanking the G-quadruplex motif are found to significantly promote the DNAzyme function of this G-quadruplex. Accordingly, this base-pairing duplex was utilized to direct the two model DNAs to fold into different bimolecular G-quadruplex structures. Spectroscopic analysis shows that these quadruplex/duplex DNA structures have similar affinities for hemin binding, whereas their DNAzyme functions are entirely different, owing to the difference in the position of the base pairs in their structures. In particular, the three T–A base pairs appended onto the 5'-terminals of the bimolecular G-quadruplex confer the best DNAzyme function ever reported. These findings clearly reveal the relationship between the intrinsic properties (ligand-binding affinity and DNAzyme function) of a G-quadruplex and additional base pairs, and also provide a clue to the formation mechanism of the G-quadruplex-based DNAzyme. This will help us to further engineer superb DNAzymes and extend their applications to bioanalysis.

## Experimental Section

**Preparation of G-quadruplex-based DNAzymes:** Before use, all single-stranded DNAs were dissolved in the TE buffer (10 mM Tris-HCl, 0.1 mM EDTA, pH 7.4), and quantified by using UV/Vis absorption spectroscopy with the following extinction coefficients ( $\epsilon_{260\text{nm}}$ ,  $\text{M}^{-1}\text{cm}^{-1}$ ) for the nucleotides: A=15400, G=11500, C=7400, T=8700. The DNAzymes were prepared as described in our previous work<sup>[14]</sup> with a little modification. Briefly, DNAs were prepared in the TE buffer, and heated at 88°C for 10 min to dissociate any intermolecular interaction, then gradually cooled to room temperature. An equal volume of the 2× HEPES buffer (50 mM HEPES, pH 7.4, 40 mM KCl, 400 mM NaCl, 0.1% Triton X-100, 2% DMSO) was added to the DNA solutions, and the DNA sequences were allowed to fold for 40 min at room temperature. Then, an equal volume of hemin solution of same molar concentration was added, and incubated at room temperature for 2 h to form the hemin–G-quadruplex DNAzymes.

**Spectroscopic analysis:** The investigation of the G-quadruplex-based DNAzyme was performed in the ABTS–H<sub>2</sub>O<sub>2</sub> system at room temperature. Just before use, the stock solution of ABTS was diluted to 6 mM by

using the detection buffer (25 mM HEPES, pH 8.0, 20 mM KCl, 200 mM NaCl, 0.05% Triton X-100, 1% DMSO). To 980  $\mu\text{L}$  of 6 mM ABTS solution was added 10  $\mu\text{L}$  of 60 mM H<sub>2</sub>O<sub>2</sub>. To this mixture was quickly added 0.5  $\mu\text{M}$  DNAzyme (final concentration). The absorption spectra were recorded every 1 min by using a Cary 500 Scan UV-Vis-NIR Spectrophotometer (Varian, USA). The binding interactions between hemin and G-quadruplexes were investigated in the binding buffer by using UV/Vis absorption spectroscopy as well. The hemin–DNA complexes were prepared as described above.

**Binding assays:** Based on the peroxidase-like activities of hemin and hemin–aptamer complexes, a new method for the determination of the affinity ( $K_d$ ) of hemin-binding aptamers was developed by using UV/Vis absorption spectroscopy. Briefly, 0.1  $\mu\text{M}$  hemin was incubated with different concentrations of aptamers for 1 h in the aqueous buffer consisting of 5.45 mM ABTS, 25 mM HEPES (pH 8.0), 20 mM KCl, 200 mM NaCl, 0.05% Triton X-100, and 1% DMSO. Then, to 990  $\mu\text{L}$  of the hemin and aptamer mixture was added 10  $\mu\text{L}$  of 60 mM H<sub>2</sub>O<sub>2</sub> to initiate the reaction. The initial catalytic rates ( $\nu$ ) were recorded in different cases. According to the previous report,<sup>[25]</sup> a formula for  $K_d$  calculation was deduced below.

$K_d$  is generally defined by the formula given in Equation (1):

$$K_d = [\text{aptamer}][\text{hemin}]/[\text{hemin-aptamer}] \quad (1)$$

The molar fraction of bound species can be obtained from Equation (2):

$$f = (\nu_x - \nu_0)/(\nu_\infty - \nu_0) \quad (2)$$

in which  $\nu_0$ ,  $\nu_\infty$ , and  $\nu_x$  are the initial catalytic rates of uncomplexed hemin (in the absence of aptamers), fully bound hemin (in the presence of an extreme excess of aptamers), and hemin bound partially by aptamers (in the presence of appropriate concentrations of aptamers), respectively.

In a sense, the initial rate  $\nu$  can be replaced by the absorbance at 420 nm (the maximal absorption of reaction product ABTS<sup>•+</sup>) within the first minute. Thus, Equation (2) can be represented as given in Equation (3):

$$f = (A_x - A_0)/(A_\infty - A_0) \quad (3)$$

in which  $A_0$ ,  $A_\infty$ , and  $A_x$  are the absorbance at 420 nm within the first minute of analyzing uncomplexed hemin, fully bound hemin, and partially bound hemin, respectively.

The molar concentrations of each species are denoted by Equations (4)–(6):

$$[\text{hemin-aptamer}] = [\text{hemin}]_0 \times f \quad (4)$$

$$[\text{hemin}] = [\text{hemin}]_0 \times (1 - f) \quad (5)$$

$$[\text{aptamer}] = [\text{aptamer}]_0 - [\text{hemin-aptamer}] \quad (6)$$

in which  $[\text{aptamer}]_0$  and  $[\text{hemin}]_0$  are the initial concentrations of aptamer and hemin, respectively.

From the Equations (1), (3), (4), (5), and (6), the formula given in Equation (7) can be obtained for calculating  $K_d$ .

$$[\text{aptamer}]_0 = K_d(A_x - A_0)/(A_\infty - A_x) + [\text{hemin}]_0(A_x - A_0)/(A_\infty - A_0) \quad (7)$$

## Acknowledgements

This work was supported by the National Natural Science Foundation of China with the Grants 20675078 and 20735003, 973 project 2007CB714500, and the Chinese Academy of Sciences KJCX2.YW.H11.

**Keywords:** base pairs • DNAzyme • G-quadruplexes • hemin • UV/Vis spectroscopy

- [1] D. Sen, W. Gilbert, *Nature* **1988**, 334, 364–366.
- [2] W. I. Sundquist, A. Klug, *Nature* **1989**, 342, 825–829.
- [3] D. Sen, W. Gilbert, *Nature* **1990**, 344, 410–414.
- [4] M. Gellert, M. N. Lipsett, D. R. Davies, *Proc. Natl. Acad. Sci. USA* **1962**, 48, 2013–2018.
- [5] R. F. Macaya, P. Schultze, F. W. Smith, J. A. Roe, J. Feigon, *Proc. Natl. Acad. Sci. USA* **1993**, 90, 3745–3749.
- [6] D. M. Tasset, M. F. Kubik, W. Steiner, *J. Mol. Biol.* **1997**, 272, 688–698.
- [7] R. F. Macaya, J. A. Waldron, B. A. Beutel, H. Gao, M. E. Joesten, M. Yang, R. Patel, A. H. Bertelsen, A. F. Cook, *Biochemistry* **1995**, 34, 4478–4492.
- [8] M. Tsiang, C. S. Gibbs, L. C. Griffin, K. E. Dunn, L. L. Leung, *J. Biol. Chem.* **1995**, 270, 19370–19376.
- [9] R. R. Breaker, *Nat. Biotechnol.* **1997**, 15, 427–431.
- [10] D. Sen, C. R. Geyer, *Curr. Opin. Chem. Biol.* **1998**, 2, 680–687.
- [11] G. M. Emilsson, R. R. Breaker, *Cell. Mol. Life Sci.* **2002**, 59, 596–607.
- [12] P. Travascio, Y. Li, D. Sen, *Chem. Biol.* **1998**, 5, 505–517.
- [13] P. Travascio, A. J. Bennet, D. Y. Wang, D. Sen, *Chem. Biol.* **1999**, 6, 779–787.
- [14] T. Li, S. Dong, E. Wang, *Chem. Commun.* **2007**, 4209–4211.
- [15] T. Li, E. Wang, S. Dong, *Chem. Commun.* **2008**, 3654–3656.
- [16] T. Li, Y. Du, E. Wang, *Chem. Asian J.* **2008**, 3, 1942–1948.
- [17] Y. Xiao, V. Pavlov, T. Niazov, A. Dishon, M. Kotler, I. Willner, *J. Am. Chem. Soc.* **2004**, 126, 7430–7431.
- [18] V. Pavlov, Y. Xiao, R. Gill, A. Dishon, M. Kotler, I. Willner, *Anal. Chem.* **2004**, 76, 2152–2156.
- [19] D. Li, B. Shlyahovsky, J. Elbaz, I. Willner, *J. Am. Chem. Soc.* **2007**, 129, 5804–5805.
- [20] B. Shlyahovsky, D. Li, E. Katz, I. Willner, *Biosens. Bioelectron.* **2007**, 22, 2570–2576.
- [21] Y. Xiao, V. Pavlov, R. Gill, T. Bourenko, I. Willner, *ChemBioChem* **2004**, 5, 374–379.
- [22] D. J. Chinnapen, D. Sen, *Biochemistry* **2002**, 41, 5202–5212.
- [23] T. Li, L. Shi, E. Wang, S. Dong, *Chem. Eur. J.* **2009**, 15, 1036–1042.
- [24] T. L. Poulos, J. Kraut, *J. Biol. Chem.* **1980**, 255, 8199–8205.
- [25] Y. Wang, K. Hamasaki, R. R. Rando, *Biochemistry* **1997**, 36, 768–779.

Received: September 3, 2008

Revised: November 19, 2008

Published online: January 9, 2009